

# Influence of SiC addition on tribological properties of SiAlON

Awadesh Kumar Mallik<sup>a</sup>, K. Madhav Reddy<sup>b</sup>, Nurcan Calis Acikbas<sup>c</sup>, Ferhat Kara<sup>d</sup>,  
Hasan Mandal<sup>e</sup>, Debabrata Basu<sup>a</sup>, Bikramjit Basu<sup>b,\*</sup>

<sup>a</sup>Central Glass & Ceramic Research Institute, CSIR, Kolkata 700032, India

<sup>b</sup>Laboratory for Biomaterials, Department of Materials Science and Engineering, Indian Institute of Technology, IIT-Kanpur, India

<sup>c</sup>Department of Mechanical and Manufacturing Engineering, Bilecik University, Bilecik, Turkey

<sup>d</sup>Anadolu University, Department of Materials Science and Engineering, Eskisehir, Turkey

<sup>e</sup>Sabanci University, Istanbul, Turkey

Received 28 February 2011; accepted 30 March 2011

Available online 7 April 2011

## Abstract

The tribological properties of gas pressure sintered SiAlON and its composite with 18 wt% silicon carbide (SiC) against two different mating materials, i.e., alumina and SiAlON are evaluated. SiAlON and SiAlON–18%SiC composite ceramics were prepared by pressure less sintering and gas pressure sintering. Fretting wear tests were carried out under dry unlubricated ambient conditions (room temperature 23–25 °C; relative humidity 50–55%) with a load of 8 N for 45,000 cycles. Friction and wear properties of SiAlON–SiC proved better than the monolithic SiAlON. The formation of silica roll like structure on the composite worn surface was observed.

© 2011 Elsevier Ltd and Techna Group S.r.l. All rights reserved.

**Keywords:** A. Sintering; SiAlON and SiAlON–SiC composite; Hertzian contact pressures; Silica roll; Tribology

## 1. Introduction

In the view of their high temperature properties silicon nitride and its derivative SiAlON (solid solutions containing Al and O in addition to Si and N) ceramics received wider attention among various non-oxide ceramics. It is known that the densification of pure silicon nitride is extremely difficult due to the covalent nature of bonding between Si and N. Successful sintering is only possible by applying high pressure, as in hot pressing [1], or by adding a mixture of oxides (typically Al<sub>2</sub>O<sub>3</sub> and Y<sub>2</sub>O<sub>3</sub>) to form a liquid at sintering temperatures with the silicon dioxide that is invariably present on the surface of each silicon nitride particle [2]. The densification is dominated by liquid phase sintering with particle rearrangement and the solution-reprecipitation of particles. Liquid-forming oxides can also enter the silicon nitride structure by forming solid solutions, commonly referred to as β-SiAlON and α-SiAlON. Engineering applications of SiAlON ceramics include cutting tools, bearing balls and rollers, refractory parts, engine valves,

turbine vanes and blades, turbocharger rotors, ceramic knives, etc.

Several studies were carried out to assess the potential of silicon nitride based ceramics, due to its importance in tribological applications. The wear maps of several engineering ceramics, including SiAlONs are now available in the literature [6–20]. Basu et al. [3] reported friction and wear behaviour of SiAlON ceramics under fretting contacts. The wear experiments were carried out in a gross slip fretting regime with identical testing parameters (8 N, 200 μm, 10 Hz and 100,000 cycles) under ambient conditions of temperature (23–25 °C) and humidity (50–52% RH) and recorded the co-efficient of friction (COF) of 0.62 was recorded for the self-mated SiAlON couple. The same group of researchers established micro-structure–mechanical properties–wear resistance relationship of SiAlON ceramics [4]. It was found that the steady state coefficient of friction (COF) varied in a narrow window of 0.59–0.64, while the wear rates of investigated SiAlON ceramics were in the range of  $7.3 \times 10^{-6}$  to  $8.4 \times 10^{-5}$  mm<sup>3</sup>/Nm. Amutha Rani et al. [5] studied a comparison of tribological behaviour between α-SiAlON/Si<sub>3</sub>N<sub>4</sub> and Si<sub>3</sub>N<sub>4</sub>/Si<sub>3</sub>N<sub>4</sub> sliding pairs in water lubrication. A reduction in friction coefficient from 0.7 to 0.03 and a decrease

\* Corresponding author. Tel.: +91 512 2597771; fax: +91 512 2597505.

E-mail address: [bikram@iitk.ac.in](mailto:bikram@iitk.ac.in) (B. Basu).

in wear rate by two orders of magnitude were achieved under low load (9.8 N) and high speed ( $>0.54$  m/s) conditions. Lewis et al. [6] studied microstructure and property control in SiAlON containing monolithic and composite (SiAlON–TiB<sub>2</sub>) ceramics. All SiAlON ceramics showed improved wear coefficients. TiB<sub>2</sub> was shown to be beneficial to the formation of adherent tribochemical film. In the study by Holzer et al. [7], microstructure, mechanical and tribological properties of rare earth containing SiAlONs was recorded. A COF of 0.3 was achieved with a piston on plate configuration for two SiAlON ceramics with different  $\alpha/\beta$ -SiAlON ratios. Same group of researchers [8] reported the development of SiAlON ceramics for lubricated sliding applications. They concluded that under lubricated sliding with isooctane, SiAlON ceramics showed a more advantageous behaviour with respect to friction coefficients and wear than commercial silicon nitride and coarse-grained alumina. The Sliding wear behaviour of Ca  $\alpha$ -SiAlON ceramics at 600 °C in air were reported by Xie et al. [9]. Under all loading conditions from 1 MPa to 1 GPa, a constant high friction coefficient 0.6–0.8 was observed and a severe wear process was dominant, in which the sliding contact induced cracks were observed in different microstructures. The wear particles were generated along the wear track, but no tribofilm was detected. Increasing the sliding speed from 10 to 23 cm/s was found to significantly increase the wear rate. Aqueous tribological behaviour of  $\alpha$ -SiAlONs was reported by Satoh et al. [10]. Under the identical testing conditions, the friction coefficients of Si<sub>3</sub>N<sub>4</sub> and SiC against themselves in a pin-on-disk wear test are 0.1 or lower. They reported that the friction coefficient of each plate specimen had a high value of approximately 0.6–0.65 and the wear rate of all the specimens were about the same and in the range of 111–117  $\mu\text{m}/\text{h}$ . The nature of the rare-earth element did not have any significant influence on the friction coefficient and the wear rate. In their study on tribological behaviour of Dy-SiAlON ceramics sliding against Si<sub>3</sub>N<sub>4</sub> under lubrication of fluorine-containing oils, Ye et al. [11] reported lowest friction coefficient 0.065 under load of 20–80 N. The same group of researchers [12] reported that three fluorine-containing lubricants reduced friction coefficient and wear volume effectively for SiAlON ceramics, sliding against steel. Jones et al. [13] reported the efficacy of SiAlON–TiB<sub>2</sub> composite material for tribological applications (e.g. ball bearings, cutting tools, etc.). The wear behaviour was dominated by tribochemical reactions, forming oxygen rich tribofilms adhered to the discs surface. Reis et al. [14] recorded tribological behaviour of colloidal processed SiAlON ceramics, sliding against steel under dry conditions. They observed that the SiAlON ceramics exhibited a typical mild wear ( $10^{-6} \text{ mm}^3 \text{ N}^{-1} \text{ m}^{-1}$ ) and the dominant wear mechanisms were adhesion and abrasion. Zhang et al. reported the friction and wear behaviour of (Ca,Mg)-sialon/SAE 52100 steel pair under the lubrication of various polyols as water-based lubricating additives [15,16].

In all the above available cited research papers, SiAlON monolithics were used to evaluate their tribological behaviour, except the study of Basu et al. [17] and Lewis et al. [10]. Basu et al. observed a COF value of 0.48 and the wear volume was

$1.8 \times 10^{-5} \mu\text{m}^3$  for a SiAlON–TiB<sub>2</sub> (60/40) composite. Recently, Souza et al. [18] reported development of  $\alpha$ -SiAlON:SiC ceramic composite by liquid phase sintering with interesting properties. In this study, we prepared SiAlON composite by addition of different  $\beta$ -SiC powder contents (0–20 wt%), to Si<sub>3</sub>N<sub>4</sub>–AlN–RE<sub>2</sub>O<sub>3</sub> powder mixtures. Here, we report the fretting wear behaviour of SiAlON monolithic and SiAlON composite with SiC. The wear mechanisms were investigated and qualitative information on the wear and friction behaviour is provided.

## 2. Experimental details

### 2.1. Sample preparation

SiAlON ceramics due to good mechanical and chemical properties are used in wear applications. But their use has been limited due to high powder and processing cost until now. In order to solve this problem, low cost refractory grade  $\beta$ -Si<sub>3</sub>N<sub>4</sub> powder was attempted to produce SiAlON ceramics. Starting particle size of  $\beta$ -Si<sub>3</sub>N<sub>4</sub> powder was  $\sim 4 \mu\text{m}$ . Attrition milling was performed in isopropyl alcohol by using Si<sub>3</sub>N<sub>4</sub> balls to decrease the average particle size of  $\beta$ -Si<sub>3</sub>N<sub>4</sub> starting powder to 0.8  $\mu\text{m}$ . After milling, the slurry was dried using rotary evaporator at 40 °C. To utilize the hardness of  $\alpha$ -SiAlON and toughness of  $\beta$ -SiAlON, 30 $\alpha$ :70 $\beta$  SiAlON compositions were designed using Y–Sm–Ca multi cation doping as sintering additives according to a previous study [19]. The addition of 18 wt% SiC to monolithic composition was made to improve the hardness of SiAlON phase and the sample is coded as B0.8 + 18SiC (*composite*).

The SiC added composition (B0.8 + 18SiC) was sintered by gas pressure sintering with 10 MPa nitrogen gas pressure at 1940 °C for 2 h. The monolithic composition (SiAlON without SiC is coded as B0.8) was sintered by pressureless sintering route at 1800 °C for 1 h. The post-sintering heat treatment was performed at 1900 °C for 3 h with 1 bar nitrogen gas pressure to facilitate grain growth for only B0.8 composition and this heat treated sample is designated as a HT-B0.8. The polished surfaces of the sintered samples were coated with a thin gold–platinum layer, prior to examining using scanning electron microscope.  $\alpha/\beta$ -SiAlON phase ratio and phase composition of the intergranular phase were determined by comparison of relative intensities of X-ray diffraction (XRD) peaks (Rigaku Rint 2000, Tokyo, Japan) and structure factor, which has been described elsewhere [7]. The mechanical properties, in particular hardness and indentation fracture toughness, were determined by indentation technique. The mirror polished surfaces were indented by applying a load of 10 kg for 10 s using Vickers hardness tester. At least 5 indentations were made for each sample. The Vickers hardness (HV) was calculated using the following expression [20]:

$$\text{HV}_{10} = \frac{0.47P}{a^2} \quad (\text{i})$$

where,  $\text{HV}_{10}$  is the Vickers hardness,  $P$  is load applied and  $a$  is half the length of the diagonal of the indentation produced by the indenter.

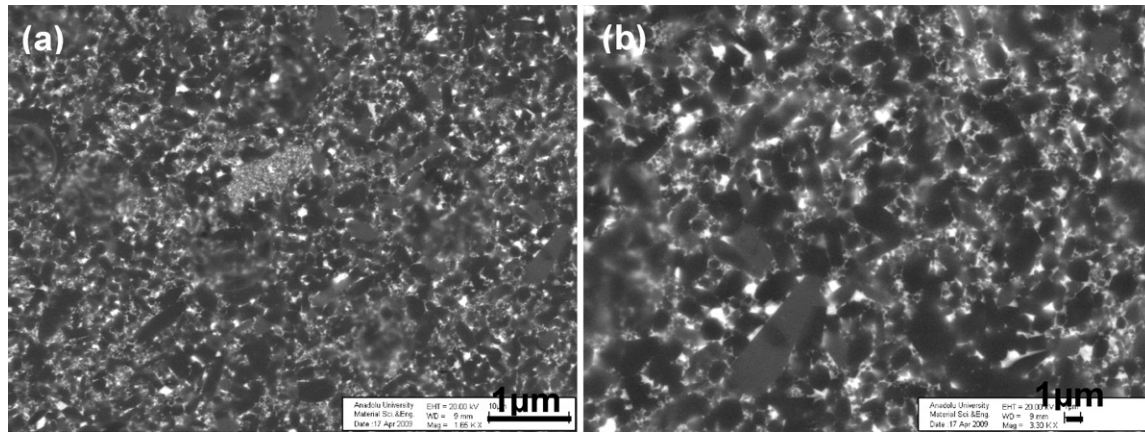


Fig. 1. SEM images of SiAlON–SiC composite samples (a) low magnification and (b) higher magnification showing different phases.

## 2.2. Wear tests and characterization

The fretting experiments were performed on a computer controlled tribometer (TR-281M, DUCOM, India) under dry unlubricated ambient conditions (room temperature 23–25 °C; relative humidity 50–55%). The details of the experimental set up can be found elsewhere [21]. Prior to the wear experiments, the flat samples of B0.8 + 18SiC composite and HT-B0.8 were ground and smoothly polished down to average surface roughness ( $R_a$ ) of less than 0.05  $\mu\text{m}$ . The counter bodies (alumina and SiAlON) are 6 mm and 10 mm balls with average surface roughness ( $R_a$ ) of 0.02  $\mu\text{m}$ . All the experiments were conducted at constant load (8 N) with an oscillating frequency of 5 Hz and 100  $\mu\text{m}$  linear stroke for duration of 45,000 cycles. The wear scar profiles on each sample were obtained using a computer controlled Laser Surface Profilometer (Mahr-Perthometer PGK 120, Germany). 2-D wear scar profiles were extracted from different locations on 3-D profiles and the wear volumes were calculated by integrating the surface area of each 2-D profile over the distance of worn surfaces. From the estimated wear volume, the specific wear rate was calculated using the following formula:

$$\text{Wear rate} = \frac{\text{Wear volume}}{\text{load} \times \text{total fretted distance}} \quad (\text{ii})$$

In order to identify the dominant wear mechanisms, the worn surfaces were examined using FE-SEM, which is equipped with energy dispersive X-ray spectroscopy (EDS).

## 3. Results and discussion

### 3.1. Material characterisation

The mechanical and microstructural characterization were carried out on monolithic SiAlON ceramic and SiAlON SiC composite. Figs. 1 and 2 show the microstructure of the B0.8 + 18SiC composite and heat treated monolithic HT-B0.8 ceramic, respectively. The microstructure of HT-B0.8 ceramic consists of predominantly 0.5–2  $\mu\text{m}$  sizes  $\alpha$ - and  $\beta$ -SiAlON grains, which are equiaxed in nature but some elongated grains with aspect ratio of 4–6 are also present (Fig. 1). When heat treatment at 1900 °C for 3 h was applied to SiAlON, no marked difference was observed in the microstructure. In develop self-reinforced microstructure after heat treatment, the grain size of SiAlON after sintering should have been fine, preferably less than 0.5  $\mu\text{m}$ . Otherwise, coarse grains, even around 0.8  $\mu\text{m}$ , do not have enough driving force for grain growth [23]. SEM images of B0.8 + 18SiC sample reveal the presence of fine (0.2–0.4  $\mu\text{m}$ )  $\alpha$ - and  $\beta$ -SiAlON grains and some elongated

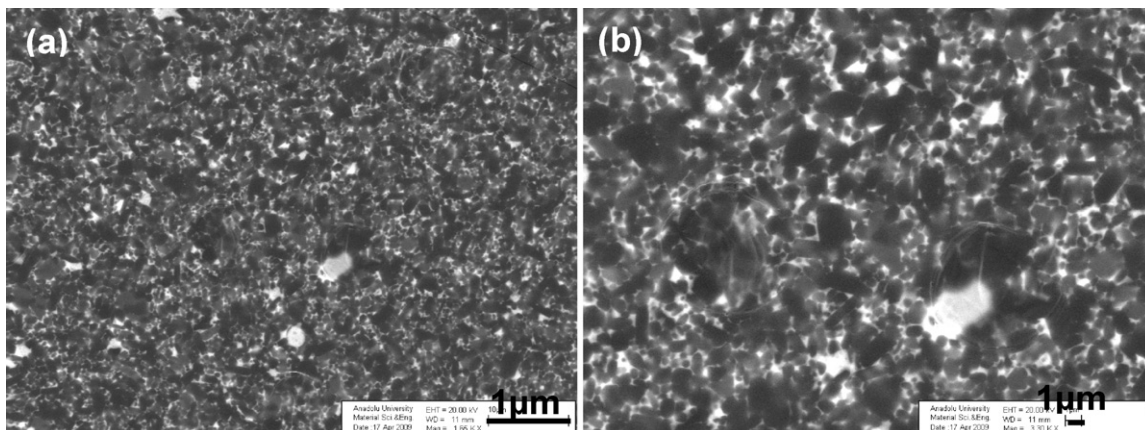


Fig. 2. SEM images of monolithic SiAlON samples (a) low magnification and (b) higher magnification showing different phases.



Table 1

Composition and mechanical properties of the SiAlON–18%SiC composite and monolithic SiAlON ceramics to be used in fretting wear.

Sample	Density (kg/m <sup>3</sup> )	HV <sub>10</sub> (GPa)	K <sub>IC</sub> (MPam <sup>1/2</sup> )	XRD
HT-B0.8 (monolithic)	3.4	14.0 ± 0.13	4.2 ± 0.1	81β:19αM:0.39
B0.8 + 18SiC (composite)	3.3	15.6 ± 0.12	5.1 ± 0.1	68β:32αM:0.46β-SiC

Table 2

Counter-body properties, according to the supplier.

Ball material	Hardness (GPa) at 5 kg load	Toughness (MPam <sup>1/2</sup> )	Roughness (μm)	Elastic modulus (GPa)
Alumina (99.7% pyre, Grade 10)	19	4.0	0.02	300
Si <sub>6–Z</sub> Al <sub>2</sub> O <sub>2</sub> N <sub>8–Z</sub> Z = 0.3, Grade TCQ	15.5	4.7	0.02	310

grains with a aspect ratio 4–8 (Fig. 2). α:β-SiAlON phase ratio and phase composition of the intergranular phase were determined using X-ray diffraction (XRD) analysis. Such analysis showed that the final phase composition of the B0.8 + 18SiC composite had around 68% β-SiAlON and 32% α-SiAlON, and 0.46% melilite phase in addition to β-SiC. On the other hand, final phase composition of HT-B0.8 sample had around 81% β-SiAlON and 19% α-SiAlON, and 0.39% melilite phase.

The recorded hardness (HV<sub>10</sub>) and fracture toughness (K<sub>IC</sub>) values of composite and monolithic ceramics ranged from 15.6 ± 0.12 GPa to 14.0 ± 0.13 GPa and 5.0 ± 0.08 MPam<sup>1/2</sup> to 4.2 ± 0.06 MPam<sup>1/2</sup>, respectively, which shows that SiAlON ceramics after SiC addition provides better hardness and fracture toughness, as summarised in Table 1. Souza et al. [18] reported a hardness (HV<sub>2</sub>) value of about 15 GPa and fracture toughness K<sub>IC</sub> of about 4.5 MPam<sup>1/2</sup> for SiAlON composite containing 15% SiC, which are almost similar to our experimental findings with SiAlON ceramics containing 18% SiC in the present case.

### 3.2. Tribological properties

The materials were ultrasonically cleaned with acetone prior to the fretting experiment. Detailed mechanical and physical properties of the mating materials are provided in Table 2. Fig. 3 shows the schematic of fretting experimental conditions. Fig. 4 shows that there was an initial running-in-period of 400–700 cycles, after which the steady state friction values were achieved. Table 3 depicts the wear and friction values of all the experiments and will be analysed later.

In our experiment the reason behind choosing alumina counterbody was to have harder material fretting against SiAlON ceramics. The SiAlON balls were chosen to study tribological properties of self-mated systems. Two different Al<sub>2</sub>O<sub>3</sub> ball sizes of 6 and 10 mm were used to realise different Hertzian contact pressure at fretting contacts.

Hertzian contact pressure ( $P_o$ ) was calculated using the following set of equations [22]:

$$P_o = \frac{3}{2} P_m = \frac{6WE^{*2}}{\pi^3 R^2} \quad (1)$$

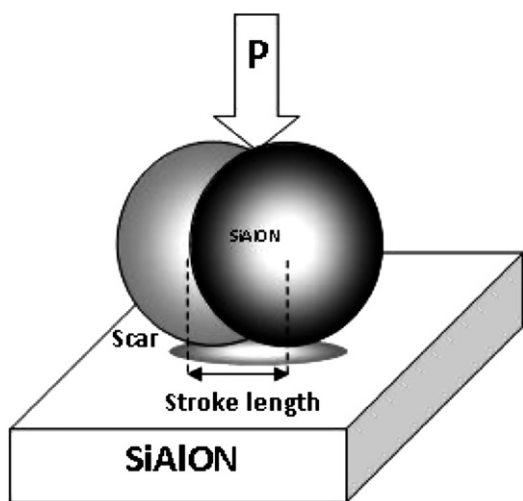


Fig. 3. Schematic of fretting test conditions: Hertzian contact stress: ≈1120 MPa & ≈800 MPa, constants – stroke length 100 μm, oscillation frequency 6 Hz, number of cycles (45,000) and normal load (8 N).

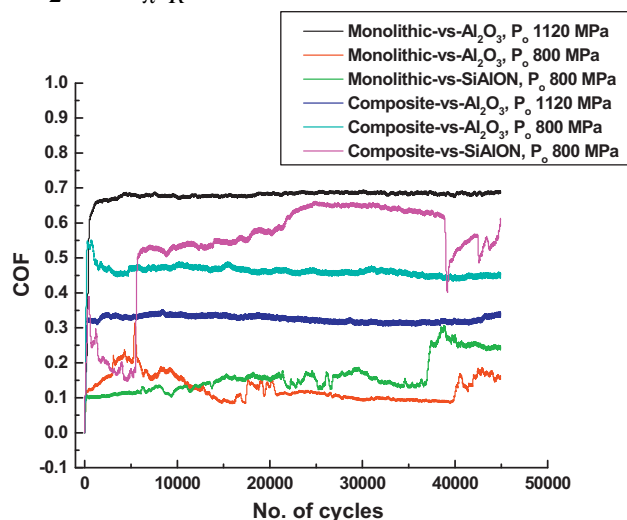


Fig. 4. Plot showing the variation of co-efficient of friction (COF) with fretting duration (as number of cycles) during fretting of against two different counterbodies such as SiAlON and Al<sub>2</sub>O<sub>3</sub> with monolithic and composite materials. Fretting conditions: 8 N load, 6 Hz frequency, 45,000 cycles and 100 μm stroke length.

Table 3

Hertzian contact pressure, wear &amp; COF values of fretting wear couples.

Wear couple	Hertzian contact pressure, $P_o$ (MPa)	Steady state COF	Wear volume ( $\text{mm}^3$ )	Wear rate ( $\text{mm}^3/\text{Nm}$ )
Composite-vs- $\text{Al}_2\text{O}_3$	1130	0.55	$7.2 \times 10^{-4}$	$1.0 \times 10^{-5}$
Composite-vs- $\text{Al}_2\text{O}_3$	800	0.15–0.2	$6.1 \times 10^{-4}$	$8.4 \times 10^{-6}$
Composite-vs-SiAlON	810	0.3–0.35	$3.1 \times 10^{-4}$	$4.3 \times 10^{-6}$
Monolithic-vs- $\text{Al}_2\text{O}_3$	1110	0.69	$1.4 \times 10^{-3}$	$2.0 \times 10^{-5}$
Monolithic-vs- $\text{Al}_2\text{O}_3$	790	0.15–0.25	$1.2 \times 10^{-3}$	$1.7 \times 10^{-5}$
Monolithic-vs-SiAlON	800	0.15–0.25	$1.6 \times 10^{-4}$	$2.2 \times 10^{-6}$

The initial contact diameter is given by,

$$a = \left( \frac{3WR}{4E^*} \right)^{1/3} \quad (2)$$

where  $W$  is the applied load,  $E^*$  is effective elastic modulus and  $R$  is the radius of the ball.

Based on the above analysis Hertzian contact pressures turn out to be  $1120 \pm 10$  MPa with initial contact diameter of  $50 \mu\text{m}$  for 6 mm diameter ball and  $800 \pm 10$  MPa with initial contact diameter of  $60 \mu\text{m}$  for 10 mm diameter ball, respectively. For a given load of 8 N, as the ball diameter increased from 6 mm to 10 mm, initial contact diameter increased from  $50 \mu\text{m}$  to  $60 \mu\text{m}$ , which thereby reduced Hertzian contact pressure  $P_o$ .

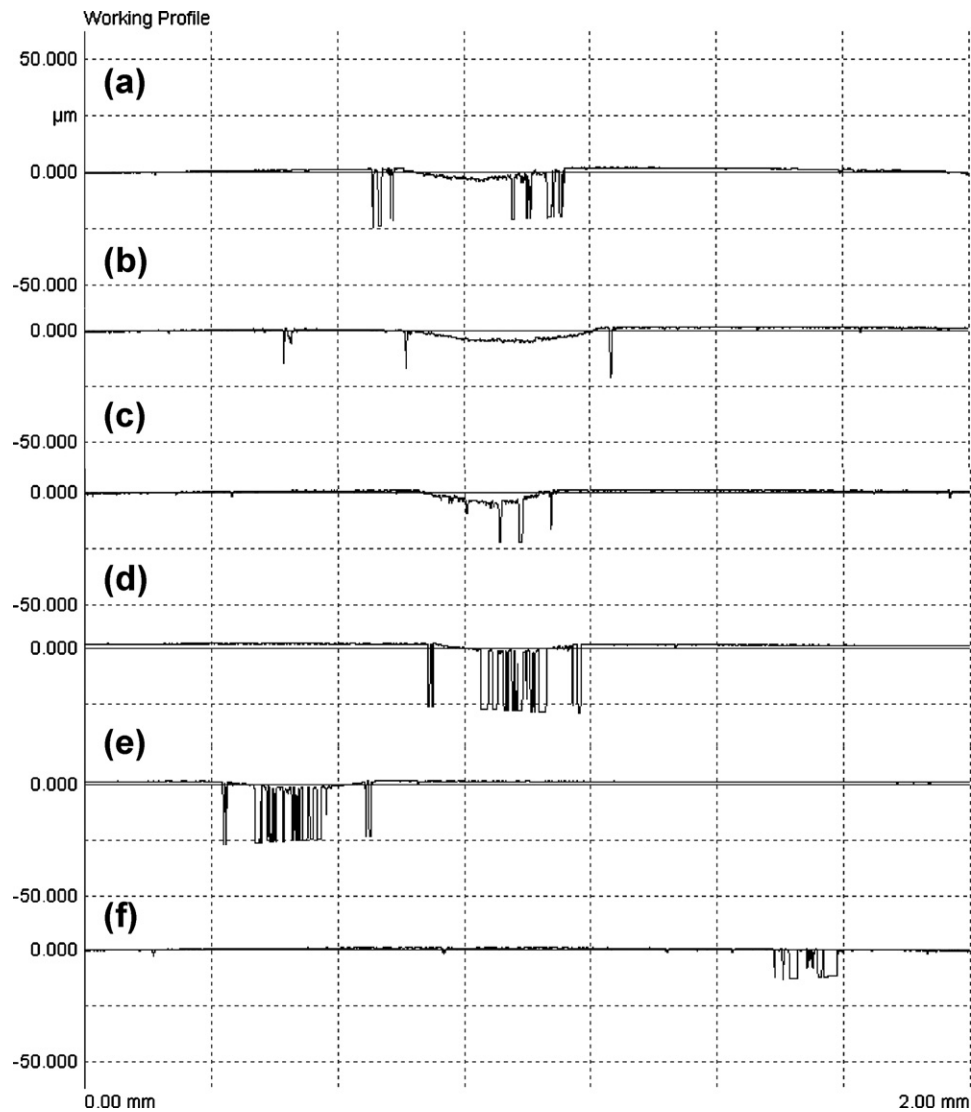


Fig. 5. 2D surface profiles, measured using laser surface profilometer of worn surfaces on various investigated materials after testing against alumina and SiAlON balls with 1120 MPa and 800 MPa Hertzian contact stresses. (a) Composite-vs-Alumina ( $P_o = 1120$  MPa), (b) composite-vs-Alumina ( $P_o = 800$  MPa), (c) composite-vs-SiAlON ( $P_o = 800$  MPa), (d) monolithic-vs-Alumina ( $P_o \approx 1120$  MPa), (e) monolithic-vs-Alumina ( $P_o \approx 800$  MPa), and (f) monolithic-vs-SiAlON ( $P_o \approx 800$  MPa). Fretting conditions: 45,000 cycles, 6 Hz frequency, 8 N load, and  $100 \mu\text{m}$  stroke length.

from about 1120 MPa to about 800 MPa. Therefore fretting tests with  $\text{Al}_2\text{O}_3$  were carried out under the two Hertzian contact pressures of  $P_o \approx 1120$  MPa and  $P_o \approx 800$  MPa.

It was found that the SiAlON monolithic/alumina couple ( $P_o = 1120$  MPa) exhibited average steady state COF of 0.55, when fretted against B0.8 + 18SiC composite flats. In contrast, average COF of 0.69 with HT-B0.8 monolithic SiAlON flat-vs-Alumina ball ( $P_o = 1120$  MPa) wear couple was obtained. These values are within the ranges of reported literature data [6,7]. With alumina balls at Hertzian contact pressure ( $P_o$ ) of 800 MPa against B0.8 + 18SiC composite flats and monolithic SiAlON, an average steady state friction value of 0.15–0.20 and 0.15–0.25 were recorded, respectively. A comparison of the results with SiAlON balls ( $P_o = 800$  MPa), we found that with B0.8 + 18SiC composite flats, average COF of 0.3–0.35 was

obtained and with HT-B0.8 monolithic SiAlON flats (self-mating), lower COF of 0.15–0.25 were recorded. Fig. 5 is the extracted 2D wear depth profiles out of 3D profiles for each fretting experiment. It reveals that typical wear scar depth was around 18–20  $\mu\text{m}$ . As reported in Table 3, the wear volume was  $1.636 \times 10^{-4} \text{ mm}^3$  with monolithic SiAlON-vs-SiAlON fretting couple (self mating & with  $P_o \approx 800$  MPa). We obtained almost similar value,  $3.1 \times 10^{-4} \text{ mm}^3$  with B0.8 + 18SiC composite flat-vs-SiAlON ball ( $P_o \approx 800$  MPa). Such wear volume was reproducible with alumina counterbodies at 800 MPa Hertzian contact pressure. Strikingly, one order of higher wear volume,  $1.25 \times 10^{-3} \text{ mm}^3$  was obtained with HT-B0.8 monolithic SiAlON flat-vs-Alumina ball couple ( $P_o \approx 800$  MPa). The wear volume of  $1.45 \times 10^{-3} \text{ mm}^3$  was obtained, when HT-B0.8 monolithic

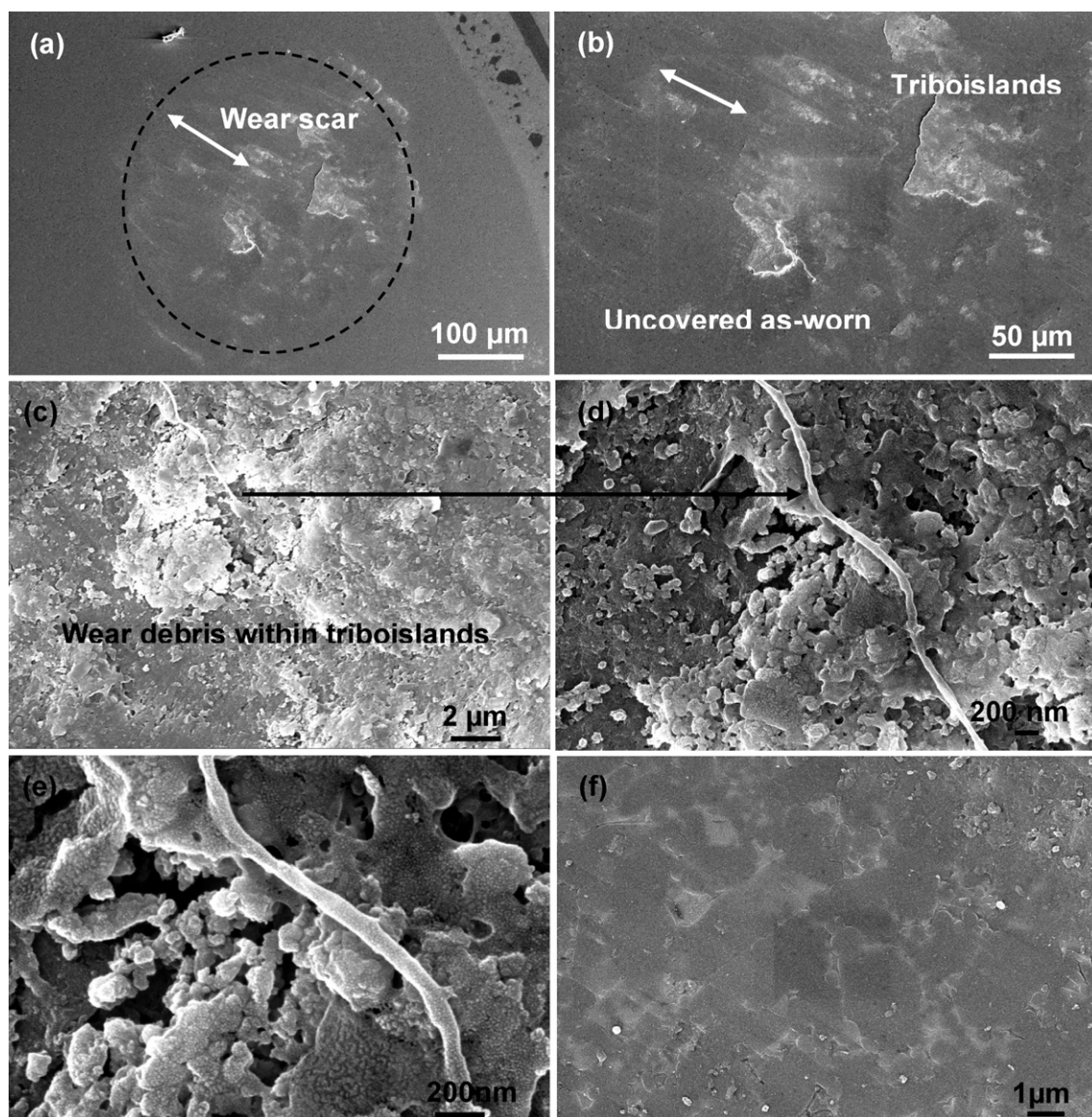


Fig. 6. SEM images revealing the overview and detailed topographical features of the as-worn surfaces of B0.8 + 18SiC composite ceramic after 45K cycles with least wear rate (a) overall view of wear track (Fig. 9b is the optical micrograph of the same area), (b) triboislands inside the scar, (c) wear debris within triboisland, and (d) silica roll along with wear debris on the triboisland, (e) magnified view of hydrated silica gel, (f) uncovered as-worn surface showing typical SiAlON microstructure along with wear debris particles and wear grooves. Doubly pointed arrow marks indicate the fretting direction. Fretting conditions: 8 N load, 6 Hz frequency, 100  $\mu\text{m}$  stroke length; Hertzian contact pressure of  $P_o \approx 800$  MPa.



SiAlON was fretted against Alumina ball ( $P_o \approx 1120$  MPa). But this was not found with B0.8 + 18SiC composite flats, fretted against alumina balls at Hertzian contact pressure of 1120 MPa. The values were much lower in the order of  $7.25 \times 10^{-4}$  mm<sup>3</sup>. The reason again is the high hardness of SiC containing composite material compared to pure monolithic SiAlON ceramics. Wear volume did not reduce much when composites with high hardness were fretted against alumina balls with about 1120 MPa contact pressure. To summarize the wear results, it can be said that under unlubricated conditions, SiC reinforced composite material behave better than pure monolithic SiAlON ceramics, except self-mating conditions. Typical wear rates varied from  $2.27 \times 10^{-6}$  to  $2.02 \times 10^{-5}$  mm<sup>3</sup> N<sup>-1</sup> m<sup>-1</sup>. A ranking of the different wear couples in terms of increasing wear rate is as

follows, self mated monolithic SiAlON at  $P_o \approx 800$  MPa > SiAlON–SiC composite-vs-SiAlON at  $P_o \approx 800$  MPa > SiAlON–SiC composite-vs-Alumina at  $P_o \approx 800$  MPa > SiAlON–SiC composite-vs-Alumina at  $P_o \approx 1120$  MPa > SiAlON monolithic-vs-Alumina at  $P_o \approx 800$  MPa > SiAlON monolithic-vs-Alumina with  $P_o \approx 1120$  MPa. We can conclude that SiAlON ceramics with 18 wt% SiC can exhibit better tribological property under fretting contact than self-mating tribocouple.

### 3.3. Microstructure-wear property correlation

Fretting occurs due to low amplitude oscillatory motion in the tangential direction (ranging from few tens of nanometers to a few tens of micrometers) at the contacting surfaces. This is a

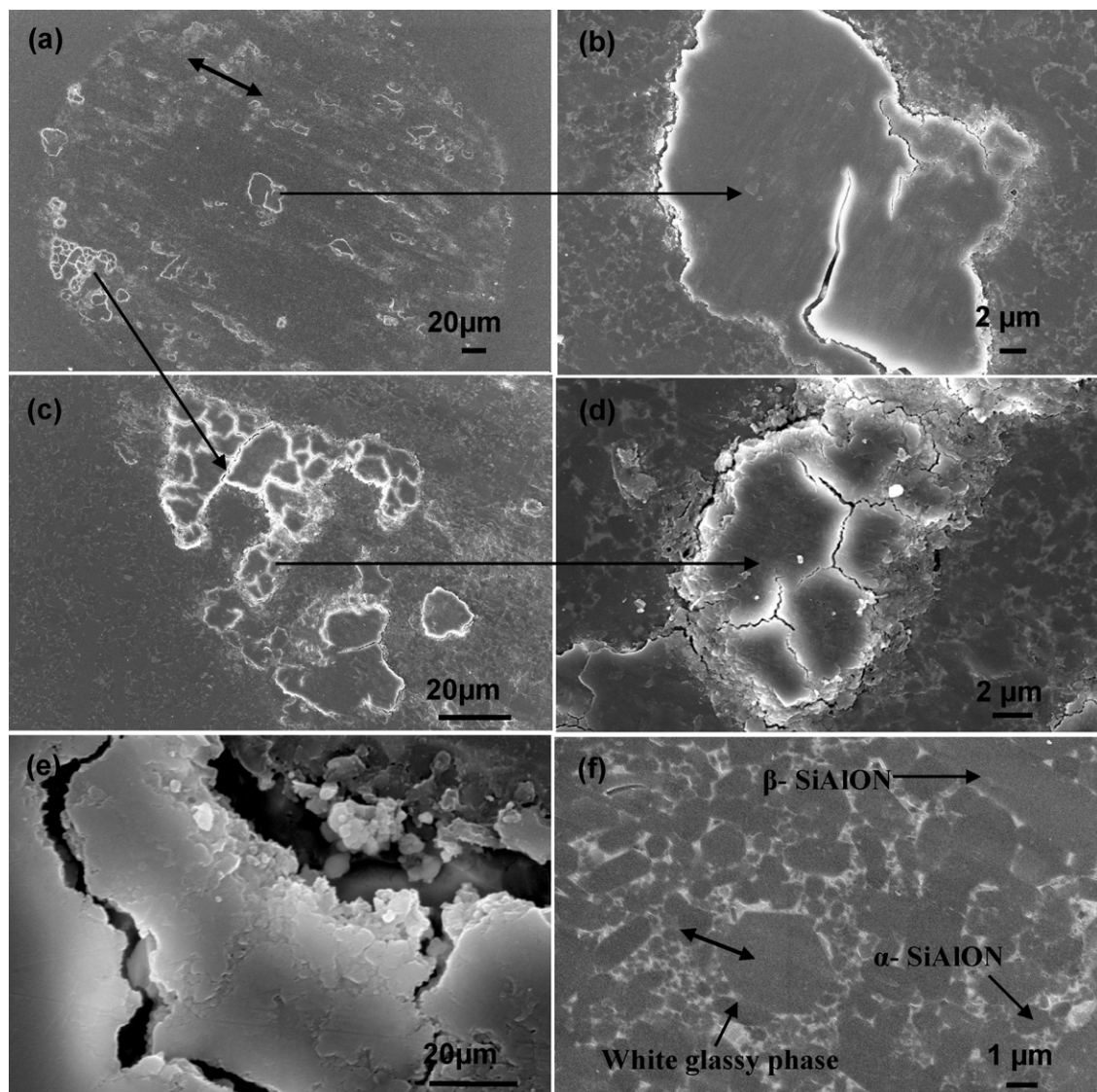
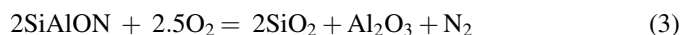


Fig. 7. SEM images revealing the overview and detailed topographical features of the as-worn surfaces of B0.8 + 18SiC composite ceramic after 45K cycles with maximum wear rate (a) overall view of the wear track showing island formation and uncovered surfaces (Fig. 9a is the optical micrograph of the same area), (b) magnified view of the central triboisland showing crack propagation and thereby fragmentation of triboislands, (c) typical fragmented triboisland, (d) magnified view of (c). (e) Spalling triboislands leads to creation of wear debris, (f) uncovered as-worn surface showing typical SiAlON microstructure along with wear grooves, doubly pointed arrow marks indicate the fretting direction. Fretting conditions: 8 N load, 6 Hz frequency, 100 μm stroke length; Hertzian contact pressure of  $P_o \approx 1120$  MPa.

form of adhesive and abrasive wear, where normal load causes adhesion between asperities and oscillatory movement causes ruptures, resulting in wear debris. Fig. 6 shows the overview and detailed topographical features of the as-worn surfaces after 45,000 cycles. The formation of triboislands at the central regions can be observed. A closer look at the triboislands inside the scar in Fig. 6(b–d), reveals that these triboislands contain wear debris particles. An interesting feature is a thread like structure, which is nothing but silica roll (Fig. 6d, e), typical of silicon carbide worn samples [23,24]. The thread or roll like structure forms due to hydration of silica, inherently present on the surface of SiAlON due to oxidation. When  $\text{SiO}_2$  comes in contact with atmospheric moisture, it becomes hydrated silica gel under the action of heat and stress. Fig. 6f is the magnified view of uncovered as-worn surface, showing typical microstructure along with wear debris particles and wear grooves. All wear scars are characterised by deep abrasive grooves of 8–20  $\mu\text{m}$  or more width (Figs. 6 and 7). EDAX peaks (Fig. 8) indicate evidence for silica layer formation, while less intense oxygen peak from as-worn surface (without any triboisland) was detected.

Fig. 7a shows the overview and detailed topographical features of the as-worn surfaces of composite ceramic after 45,000 cycles. Abrasive wear produces oxygen-rich hard wear

particles, which are present all over the grooves. These particles form tribolayer under combined action of heat and stress. The tribolayer formation is a dynamic process. Oxidation of abrasive wear particles takes place probably by the following reaction:



Grain pull-out is also seen on the wear track. One typical feature of fragmentation of triboisland was the interaction of cracks on worn surface (see Fig. 7c, d). Fig. 7e reveals spalling of triboislands due to crack propagation. Such a spalled layer under the fretting action leads to wear debris formation along the edge of islands. Fig. 7f is the magnified view of as-worn surface (not covered with triboisland), showing typical SiAlON microstructure (equiaxed  $\alpha$ -SiAlON grains and elongated  $\beta$ -SiAlON grains and intergranular white glassy phases) along with wear grooves. The width of the abrasive wear grooves vary from few microns to 20  $\mu\text{m}$  or more. These wider grooves are due to ploughing action by harder alumina counter body (19 GPa).

SiC is quite stable and does not undergo oxidation at lower temperatures. However, during wear, under combined mechanical and chemical processes, the degradation process becomes more profound. Yumamoto and Ura studied the dry sliding wear

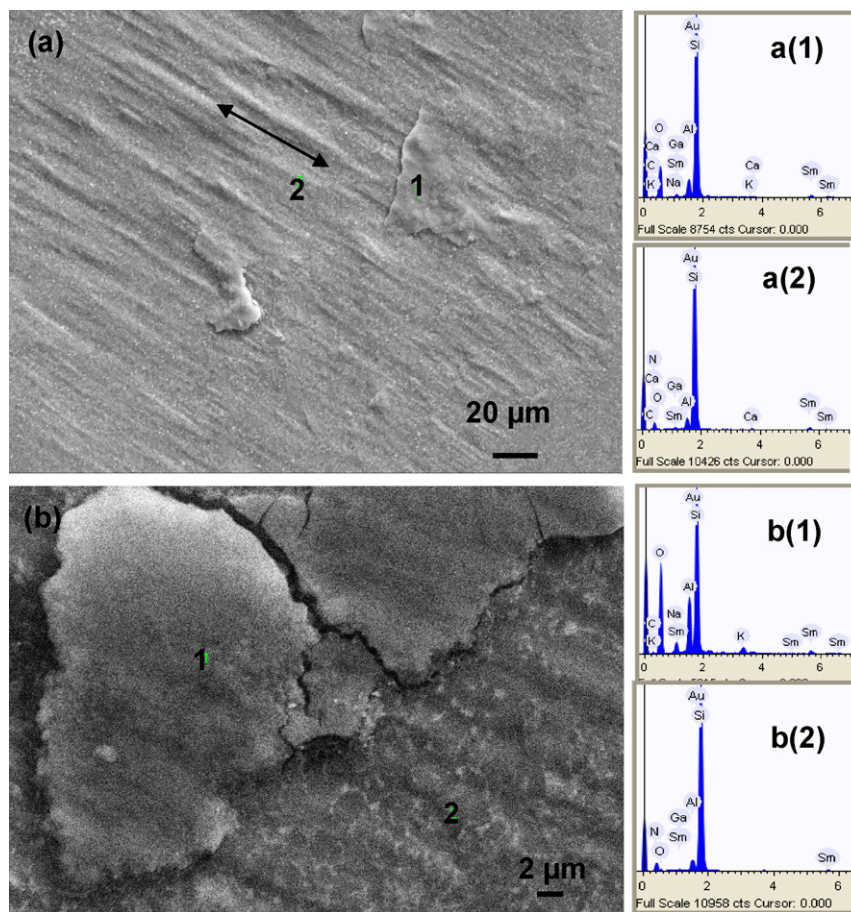


Fig. 8. SEM images of abrasive grooves on (a) composite flat-SiAlON ball wear couple (with  $P_o \approx 800$  MPa) and (b) composite flat-alumina ball wear couple (with  $P_o \approx 1120$  MPa) with EDAX signals from respective places of silica rich tribolayer (a1, b1) and unlayered wear track (a2, b2). Doubly pointed arrows indicate the fretting direction.



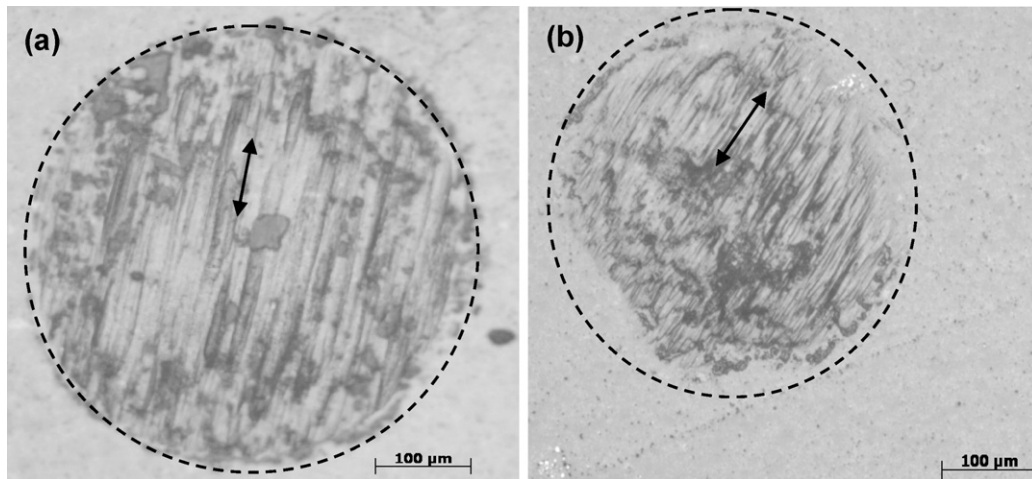


Fig. 9. Optical Micrograph of wear scar (a) SiAlON–SiC composite flat-on-Alumina ball couple with  $P_o \approx 1120$  MPa. Diameter of wear scar is 580  $\mu\text{m}$ , (b) SiAlON–SiC composite flat-on-SiAlON ball couple  $P_o \approx 800$  MPa. Diameter of wear scar is 400  $\mu\text{m}$ . Double arrow indicates reciprocating direction and dotted circle estimates the wear scar diameter.

of SiC with different environments conditions (Argon, Nitrogen and air) and it was noticed that in presence of air, SiC got oxidised to silica and the coefficient of friction (COF) drastically decreased from 0.8 to 0.3 [25]. Andersson and Blomberg also carried out wear tests in air and arrived at a similar conclusion [26]. Takadoun et al. pointed out that the fall of friction coefficient was due to the formation of hydrated silica [27]. The silica gel, being soft in nature, reduces the friction coefficient and progressively the tribo-surfaces become very smooth. The similar reactions were identified in liquid medium (i.e., water) [28]. After the running-in-period, the oxide debris generated was removed and the test was continued. However the friction coefficient increased again due to removal of silicon oxide debris. In our study, silica rolls are observed to be quite stable and COF of friction remained constant until the end of the fretting cycles (see Figs. 4 and 6). Interestingly, it is also noticed in SiAlON composite, even at high contact pressure ( $P_o \sim 1120$  MPa), COF is comparatively lower than the low contact pressure ( $P_o \sim 800$  MPa) as against  $\text{Al}_2\text{O}_3$  mating materials. The plausible reason could be the formation of silica gel.

We started fretting experiment with a 100  $\mu\text{m}$  stroke length and maximum semi-contact width for Hertzian contact pressure of  $P_o \approx 800$  MPa was 70  $\mu\text{m}$ . So at the extreme position when the ball was at the one end of stroke length, the contacting surfaces would be another 70  $\mu\text{m}$  away in the same stroke direction. Considering this, we can say for contact pressure  $P_o \approx 800$  MPa, with stroke length of 100  $\mu\text{m}$ , the effective wear scar mark would be of 240  $\mu\text{m}$  along the fretting direction. But we find from Fig. 9b that wear scar mark for  $P_o \approx 800$  MPa is only 300  $\mu\text{m}$  along the fretting direction and 400  $\mu\text{m}$  perpendicular to it. This is typical feature of partial slip, characterised by low wear and oxidation, often known as “fretting fatigue”. We can conclude that fretting at  $P_o \approx 800$  MPa results in less wear scar diameter along the stroke direction

than perpendicular direction due to partial slip. On the other hand, the wear scar diameter (at  $P_o \approx 1120$  MPa) is 580  $\mu\text{m}$  along fretting direction, and 470  $\mu\text{m}$  perpendicular to it (Fig. 9a), which is typical of gross slip condition. The essential characteristics of gross slip regime are evident in Fig. 9a with severe wear, often known as “fretting wear”.

#### 4. Conclusions

The friction and wear behaviour of SiAlON and its composites (18 wt% SiC) can be summarized as follows.

- In addition to the improvement in mechanical properties with SiC addition, COF is reduced for SiAlON–SiC ceramic composite as the steady state with narrow range 0.35–0.5 has COF been attained, when fretted against alumina ball with different Hertzian contact pressure (800 and 1120 MPa). However with the self mating materials (SiAlON ball), the friction value is significantly increased after 10,000 cycles from 0.15 to 0.65.
- The estimated wear rate for monolithic SiAlON and SiAlON–SiC composite were in the similar range of  $\sim 10^{-5}$  to  $5 \times 10^{-6}$  as against two different mating materials, irrespective of Hertzian contact pressures. In contrast, SiAlON composite against the  $\text{Al}_2\text{O}_3$  ball at 800 MPa contact pressure exhibited one order magnitude of low wear rate, is measured.
- The topographical observations of the worn surfaces using SEM–EDS analysis indicate the dominance of tribomechanical wear assisted by grain pull out SiAlON counterbodies. Another observation is that harder alumina ball causes more damage than SiAlON ball under identical fretting conditions.
- At low Hertzian contact pressure ( $P_o \sim 800$  MPa) the typical feature of partial slip, characterised by low wear and oxidation, often known as “fretting fatigue” was observed.

In contrast, the typical feature of gross slip with silica rolls was observed at higher Hertzian contact pressure of 1200 MPa.

## Acknowledgments

This work was done in connection with Indo-Turkey S&T co-operation under CSIR-TUBITAK project titled “Development of SiAlON Ceramics for Tribological Applications”.

## References

- [1] G.G. Deeley, J.M. Herbert, N.C. Moore, Dense silicon nitride, *Powder Metallurgy* 8 (1961) 145–151.
- [2] K. Komeya, H. Inoue, Heat resistant strengthened composites. Japanese Patent No. 703695, 1969.
- [3] B. Basu, J. Vleugels, M. Kalin, O. Van Der Biest, *Materials and Engineering A359* (2003) 228–236.
- [4] R. Kumar, N.C. Acikbas, B. Basu, F. Kara, H. Mandal, *Metallurgical Materials Transaction A* 40A (2009) 2319–2332.
- [5] D. Amutha Rani, Y. Yoshizawa, M.I. Jones, H. Hyuga, K. Hirao, Y. Yamauchi, *Journal of the American Ceramic Society* 88 (2005) 1655–1658.
- [6] M.H. Lewis, N. Gajom, R.S. Dobedoe, A.H. Jones, *Key Engineering Materials* 237 (2003) 129–140.
- [7] S. Holzer, J.P. Hantsche, U. Spicher, B. Huchler, A. Nagel, R. Oberacker, D. Badenheim, M.J. Hoffmann, *Key Engineering Materials* 287 (2005) 282–292.
- [8] S. Holzer, J.P. Hantsche, U. Spicher, D. Badenheim, R. Oberacker, M.J. Hoffmann, *Mat.-wiss. u. Werkstofftech.* 36 (3/4) (2005) 117–121.
- [9] Z.-H. Xie, M. Hoffman, R.J. Moon, P.R. Munroe, Y.-B. Cheng, *Wear* 260 (2006) 1356–1360.
- [10] T. Satoh, K. Hirao, S. Sakaguchi, Y. Yamauchi, S. Kanzaki, *J. Mater. Sci. Lett.* 21 (2002) 97–99.
- [11] C. Ye, W. Liu, Y. Chen, Z. Ou, *Wear* 253 (2002) 579–584.
- [12] W. Liu, C. Ye, Y. Chen, Z. Ou, D.C. Sun, *Tribology International* 35 (2002) 503–509.
- [13] A.H. Jones, R.S. Dobedoe, M.H. Lewis, R.J. Lumby, W.E. Lee, B. Derby, *British Ceramic Proceedings, Annual Ceramic Convention Symposium on Engineering with Ceramics*, 1998, pp. 133–149.
- [14] P. Reis, J.P. Davim, X. Xu, J.M.F. Ferreira, *Tribology Letters* 18 (3) (March 2005).
- [15] W.G. Zhang, W.M. Liu, H.W. Liu, L.G. Yu, *Tribology International* 33 (2000) 769–775.
- [16] W.G. Zhang, W.M. Liu, H.W. Liu, L.G. Yu, Q.J. Xue, *Wear* 223 (1998) 143.
- [17] B. Basu, J. Vleugels, O. Van Der Biest, *Wear* 250 (2001) 631–641.
- [18] J.V.C. Souza, C. Santos, C.A. Kelly, O.M.M. Silva, *International Journal of Refractory Metals & Hard Materials* 25 (2007) 77–81.
- [19] N. Calis Acikbas, R. Kumar, F. Kara, H. Mandal, B. Basu, Influence of  $\beta$ -Si<sub>3</sub>N<sub>4</sub> particle size and heat treatment on microstructural evolution of  $\alpha$ : $\beta$ -SiAlON ceramics.
- [20] A.G. Evans, E.A. Charles, Fracture toughness determinations by indentation, *Journal of the American Chemical Society* 59 (1976) 371–372.
- [21] H. Mohrbacher, J.P. Celis, J.R. Roos, *Tribology International* 28 (5) (1995) 269–278.
- [22] B.R. Lawn, *Fracture of Brittle Solids*, Second Edition, Cambridge University Press, 1993,, p. 254.
- [23] V.S.R. Murthy, H. Kobayashi, N. Tamari, S. Tsurekawa, T. Watanabe, K. Kato, *Wear* 257 (2004) 89–96.
- [24] J.R. Gomes, M.I. Osendi, P. Miranzo, F.J. Oliveira, R.F. Silva, *Wear* 233/235 (1999) 222–228.
- [25] Y. Yamamoto, A. Ura, *Wear* 154 (1992) 141–150.
- [26] P. Andersson, A. Blomberg, *Wear* 174 (1994) 1–7.
- [27] J. Takadom, Z. Zsiga, C. Roques-Carmes, *Wear* 174 (1994) 239–242.
- [28] R.S. Gates, S.M. Hsu, *Tribology Letters* 17 (2004) 399–407.